Carboxylate Ions Are Strong Allosteric Ligands for the HisB10 Sites of the R-State Insulin Hexamer

Sheng Tung Huang,‡ Wonjae E. Choi, Curtis Bloom,§ Melissa Leuenberger, and Michael F. Dunn*

Department of Biochemistry-015, University of California, Riverside, California 92521

Received January 24, 1997; Revised Manuscript Received June 10, 1997⊗

ABSTRACT: The insulin hexamer is an allosteric protein which displays positive and negative cooperativity and half-site reactivity that is modulated by strong homotropic and heterotropic ligand binding interactions at two different loci. These loci consist of phenolic pockets situated on the dimer−dimer interfaces of T−R and R−R subunit pairs and of anion sites comprising the HisB10 metal ion sites of the R_3 units of the T_3R_3 and R_6 states. In this study, we show that suitably tailored organic carboxylates are strong allosteric effectors with relatively high affinities for the R-state HisB10 metal sites. Methods of quantifying the relative affinities of ligands for these sites in both Co(II)- and Zn(II)-substituted insulin hexamers are presented. These analyses show that, in addition to the electron density on the ion, the carboxylate affinity is influenced by polar, nonpolar, and hydrophobic interactions between substituents on the carboxylate and the amphipathic protein surface of the narrow tunnel which controls ligand access to the metal ion. Since the binding of anions to the HisB10 site makes a critically important contribution to the stability of the T_3R_3 and R_6 forms of the insulin hexamer, the design of high-affinity ligands with a carboxylate donor for coordination to the metal ion provides an opportunity for constructing insulin formulations with improved pharmaceutical properties.

The insulin hexamer is an allosteric protein that exhibits negative and positive cooperativity, half-site reactivity in ligand binding, and both homotropic and heterotropic ligand binding interactions (Kaarsholm et al., 1989; Brader et al., 1991; Choi et al., 1993, 1996; Brzovic et al., 1994; Bloom et al., 1995). The T- to R-state allosteric transitions involve the interconversion of three conformational states designated T_6,[1] T_3R_3, and R_6 (Kaarsholm et al., 1989; Brzovic et al., 1994; Bloom et al., 1995; Choi et al., 1996) (Scheme 1A). The three-dimensional structures of these states (Blundell et al., 1972; Baker et al., 1988; Smith et al., 1984, 1992a,b; Derewenda et al., 1989, 1991; Dodson et al., 1993; Ciszak & Smith, 1994; Whittingham et al., 1995) and the solution properties (Kaarsholm et al., 1989; Roy et al., 1989; Brader et al., 1991; Brzovic et al., 1994; Bloom et al., 1995; Choi et al., 1993, 1996) have been well-characterized. The T to R structural transition involves conversion of residues B1−8 from an extended conformation to an α-helix. This motion causes an ∼30 Å displacement of PheB1, exposes a cryptic amphipathic pocket at each dimer interface (the phenolic pockets), creates narrow, ∼12 Å long, tunnels from the surface down to the HisB10 sites (anion binding sites), and converts the geometry of the HisB10 Zn(II) sites from octahedral to tetrahedral coordination (Scheme 1B,C). Bloom et al. (1995) have demonstrated that the allosteric transitions among T_6, T_3R_3, and R_6 can be quantitatively described by the Seydoux, Malhotra, and Bernhard (SMB) model (Seydoux et al., 1974) for cooperativity and half-site reactivity. This three-state model (Scheme 1A) postulates two concerted allosteric transitions: one between T_6 and T_3R_3 and another between T_3R_3 and R_6. Brader et al. (1991) and Bloom et al. (1995) established the existence of strong positive heterotropic interactions in the R state between the binding of anions to the HisB10 sites and the binding of neutral organic ligands to the phenolic pockets.

Structures of T_6 and T_3R_3 usually show octahedral M(II)-N_3O_3 geometries for the T_3 units comprised of three HisB10 side chains and three water molecules (Scheme 1B). The Zn(II)- or Co(II)-substituted HisB10 sites of the T_3 unit exhibit very low affinities for monovalent anions.

The HisB10 sites of the Zn(II)-, Cu(II)-, and Co(II)-substituted R_3 units of R_6 and T_3R_3 (Scheme 1B) exhibit relatively high affinities for a wide variety of small monovalent anions, and for a few neutral ligands (imidazole and organic sulfonamides) (Roy et al., 1989; Smith et al., 1984; Brader et al., 1990, 1991, 1992a,b; Brader & Dunn, 1991; Brzovic et al., 1994). These sites have distorted tetrahedral geometries made up of the three HisB10 side chains and a fourth ligand derived from the available anions present in solution (Smith et al., 1984; Roy et al., 1989; Brader et al., 1990, 1991, 1992a,b; Derewenda et al., 1989; Ciszak & Smith, 1994; Whittingham et al., 1995). The affinities of certain anions (SCN^-, N_3^-, OCN^- and certain organic

* Corresponding author: Professor Michael F. Dunn, Department of Biochemistry-015, University of California, Riverside, CA 92521. Phone: 909-787-4235. Fax: 909-787-5390. E-mail: DUNN@UCRAC1.UCR.EDU.

‡ Current address: Department of Chemistry, Brandeis University, Waltham, MA 02254-9110.

§ Current address: Department of Chemistry, California Institute of Technology, Pasadena, CA 91125.

⊗ Abstract published in *Advance ACS Abstracts,* August 1, 1997.

[1] Abbreviations: T_6, T_3R_3, and R_6, insulin hexamers with extended (T) and α-helical (R) global conformations of B-chain residues 1−8 (Kaarsholm et al., 1989); SMB, half-site reactivity (suboptimal symmetry) model for cooperativity (Seydoux et al., 1974); ^{1}H NMR, proton nuclear magnetic resonance; Zn^{2+}- and Co^{2+}-R_6, Zn(II)- and Co(II)-substituted R-state insulin hexamers; 4H3N, 4-hydroxy-3-nitrobenzoate ion; PABA, 4-aminobenzoate; Φ, relative absorbance (see Methods); K_{Dapp}, apparent dissociation constants for ligand binding to the HisB10 sites (see Methods); K_{4H3N}, the apparent dissociation constant for 4H3N (see Methods); K_D^{Obs}, apparent dissociation constant measured in competition with 4H3N (see Methods).

S0006-2960(97)00163-3 CCC: $14.00

Scheme 1: (A) Allosteric Model for the Conformational Transitions of the Insulin Hexamer Depicting the 3-Fold Symmetry Axes, of T_6, T_3R_3, and R_6, the Pseudo-2-Fold Symmetries of Dimeric Units of T_6 and R_6, and the Complete Loss of This Pseudo Symmetry in T_3R_3,[a] (B) Cartoons Showing Coordination at the HisB10 Sites of the T-State and R-State Trimeric Units of T_6, T_3R_3, and R_6,[b] (C) Stereoview Looking along the 3-Fold Symmetry Axis into the HisB10 Site of an R_3 Unit[c]

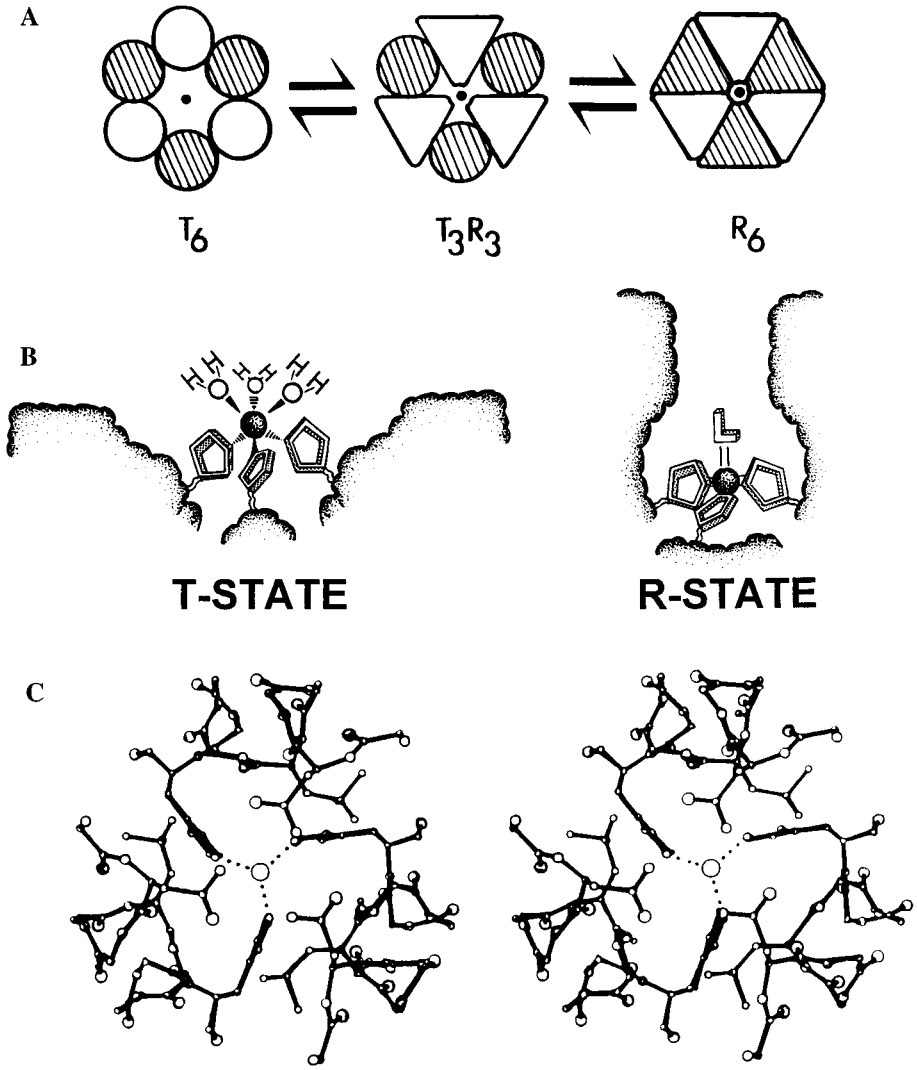

[a] T-state subunit conformations are shown as circles and R-state conformations as triangles. The alternation of striped and solid subunits represents the head-to-tail arrangement of insulin subunits in the hexamer. The HisB10 sites are represented by the black dot located on the 3-fold symmetry axis. [b] The metal sites of the T_3 units reside in shallow, dish-shaped depressions located on the 3-fold symmetry axis. The metal sites of the R_3 units are located ~12 Å below the surface at the bottom of a narrow tunnel. The T-state sites exhibit octahedral $M(II)N_3O_3$ coordination geometries (M = Zn, Co, or Cu; N = His imidazolyl; O = H_2O), while the R-state sites exhibit distorted tetrahedral or five-coordinate $M(II)N_3L$ complexes (where L = a mono- or bidentate ligand). [c] The metal ion is located at the center and is shown coordinated to the three HisB10 imidazolyl groups (dotted lines). In this conformation, the carboxamide groups of AsnB3 are positioned to form a cap over the top of the cavity [redrawn from Smith and Dodson (1992a) with permission].

carboxylates) are sufficient to stabilize R-state complexes in the absence of any ligand for the phenolic pockets (Smith et al., 1984; Kaarsholm et al., 1989; Brader et al., 1991; Brzovic et al., 1994; Bloom et al., 1995; Whittingham et al., 1995; Choi et al., 1996).

The cavity extending along the 3-fold symmetry axis from the surface down to the HisB10 metal ion site (viz. Scheme 1C) is sufficiently large to accommodate ligands as large as phenolate ion or aromatic carboxylates with small meta and para substituents. Heretofore, very little quantitative information has been published on anion affinities for this site. This report presents quantitative studies of a new class of ligands for the R-state HisB10 metal ion sites based on the organic carboxylate ion. It will be shown that carboxylates with appropriately tailored structures combine coordination to the HisB10 metal ion with weak polar and nonpolar interactions between the ligand and the amphipathic protein surface of the site to give relatively high-affinity interactions that, in conjunction with phenolic ligands, are effective in stabilizing the R_6 and T_3R_3 conformations of the insulin hexamer.

MATERIALS AND METHODS

Materials. Metal-free human insulin was a gift supplied by the Novo Research Institute (Denmark). The chemicals employed in these studies were reagent grade or better and were used as supplied. All but one of the anions were purchased from Aldrich. *m*-(Aminocarbonyl)benzoic acid was a gift from W. C. Taylor (Agriculture Research Station, Lethbridge, Canada).

Methods. Insulin monomer concentrations were determined from absorbance measurements at 280 nm using a

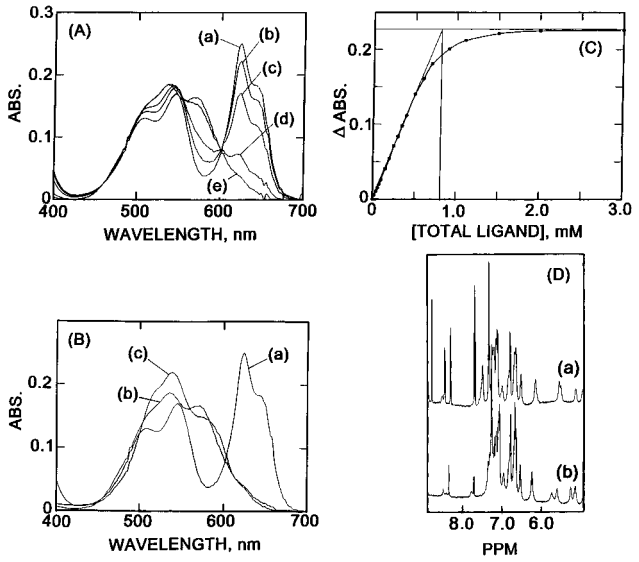

FIGURE 1: Spectroscopic signatures of carboxylate binding to the HisB10 sites of Zn(II)- and Co(II)-substituted R-state insulin hexamers. (A) UV/vis spectra of the R_6-Co(II)-substituted insulin hexamer measured in the presence of (a) 100 mM phenol (the HisB10 ligand is phenolate ion) and with additions of (b) 0.1 mM, (c) 0.5 mM, (d) 1.0 mM, and (e) 5 mM 4-aminobenzoate. (B) Effects of carboxylate structure on the d−d transitions of the Co(II)-R_6 hexamer: (a) the phenolate complex, (b) the 4-aminobenzoate complex, and (c) the valerate complex. (C) Binding isotherm for the titration of 0.34 mM Co(II)-insulin hexamer with 4H3N determined in the presence of 100 mM phenol. The *x*-intercept of the intersection between the initial and final slopes (0.71 mM) indicates a 4H3N:hexamer stoichiometric ratio of 2:1. (D) Aromatic regions of the ^{1}H NMR spectra of 0.5 mM Zn(II)-R_6 hexamer with 5 mM 3-nitrobenzoate (a) or 2 mM 3-nitro-4-hydroxybenzoate (b) coordinated to the HisB10 sites. Spectra were measured in ^2H_2O adjusted to a pH meter reading of 8.00 at 25 °C.

value for ϵ_{280} of 5700 M^{-1} cm^{-1} (Porter, 1953). The Zn^{2+}- and Co^{2+}-R_6 hexamers were prepared in Tris-$HClO_4$ buffer at pH 8.0 with a ratio of two M^{2+} ions/hexamer in the presence of 100 mM phenol. Unless otherwise stated, the conditions used for these studies are as follows: [insulin hexamer] = 0.34 mM, [phenol] = 100 mM, [Tris] = 50 mM adjusted to pH 8.00 with concentrated perchloric acid, T = 25 °C, and anionic ligands added as required by the individual experiments. The metal ion concentrations were determined by titration with the chromophoric chelator, terpy, and the signal of the titration was monitored at either 325 nm (Co^{2+}) or 330 nm (Zn^{2+}) (Holyer et al., 1966; Kaarsholm et al., 1989). Concentrated stock solutions of the carboxylic acid derivatives were dissolved in 50 mM Tris-$HClO_4$ buffer and adjusted with KOH to pH 8.0. When the anion solubility was too low in the buffer solution to allow preparation of concentrated aqueous stock solutions, ethanol (EtOH) or dimethyl sulfoxide (DMS) was used as a solvent for this purpose. Anion concentrations were confirmed by measurement of the UV/vis absorption spectrum and using extinction coefficients from published data (*Sadtler Standard Spectra*). Titration isotherms for the Co^{2+}-R_6 system were measured by adding the appropriate ligand. The replacement of phenolate ion by carboxylate anion at the metal sites of Co^{2+}-R_6 causes the spectrum to shift with disappearance of the λ_{max} peaks at 622, 542, and 510 nm (signatures of the d−d transitions of the phenolate Co^{2+}-R_6 complex) and the appearance of the carboxylate adduct spectrum (λ_{max} = 538 nm) (see Figure 1A,B) (Brader et al., 1990, 1991). The titrations reported herein were obtained by monitoring the decreasing absorbance at 622 nm as the concentration of carboxylate anion is increased. The UV/vis spectra were recorded on Hewlett-Packard 8450A and 8452A spectrophotometers. The titration curves were normalized by assuming that the saturation spectrum represents 100% displacement of phenolate by the carboxylate anion. Relative absorbance values (Φ) were used to normalize the curves to a scale ranging from 0 to 1.0 by assigning the value of absorbance at saturation as the maximum change in absorbance which can be attained and then dividing the absorbance value of each point in the titration curve by this value. The concentration of bound ligand was determined by multiplying the total metal sites in the solution by the relative absorbance. The free ligand concentration, $[L]_{free}$, was determined by subtraction of the concentration of the total ligand added from the concentration of the ligand bound. The apparent dissociation constant (K_{Dapp}) determined in these titrations measures the apparent affinity of the ligand for the HisB10 metal site in competition with phenolate ion. The hyperbolic equation (eq 1)

$$\Phi = (\Phi_{max}[L]_{free})/(K_{Dapp} + [L]_{free}) \quad (1)$$

and the computer program Peakfit (Jandel Corp.) were used to analyze the titration curves to determine the apparent dissociation constants (K_{Dapp}).

The binding isotherms for the chromophoric ligands, 4-hydroxy-3-nitrobenzoate (4H3N) and 4-nitro-3-hydroxybenzoate, were measured by titrating the ligand with a concentrated solution of the phenol-induced Zn^{2+}-R_6 hexamer. The titration signal was monitored at the more intense peak in the difference spectrum (bound minus free): λ_{max} = 444 nm for 4H3N and λ_{max} = 472 nm for 4-nitro-3-hydroxybenzoate. The chromophore, 4H3N, also was used as a spectroscopic probe in displacement studies using nine different nonchromophoric ligands to determine the titration curves for binding to the HisB10 sites of Zn^{2+}-R_6. This strategy also was used to determine the binding affinities for two inorganic anions, SCN^- and Cl^-. In this method, the signal monitors the displacement of 4H3N (decrease in absorbance at 444 nm) via competition with the nonchromophoric ligand. The experimental conditions for studying the nonchromophoric ligand employed 0.3 mM 4H3N and 0.1 mM Zn^{2+}-insulin hexamer in the presence of a saturating concentration of phenol (100 mM). The titration curves were normalized by assuming the saturation end points reached at high ligand concentrations represent 100% of the bound species. The program Peakfit was used to fit the resulting titration curves to eq 1 to determine apparent dissociation constants (K_{Dapp}). Curves were constructed from UV/vis spectra recorded on Hewlett-Packard 8450A and 8452A spectrophotometers.

^{1}H NMR spectra were measured on samples prepared as previously described (Brzovic et al., 1994). One-dimensional PRESAT spectra were collected on a GN 500 MHz spectrometer with a Nicolet 1280 computer. Spectral analyses were carried out using the software FELIX running on a Silicon Graphics computer system.

RESULTS

Ligand Binding to the Co(II)- and Zn(II)-R_6 Hexamers. The binding isotherm for the displacement of phenolate ion by 4H3N, at pH 8.0, is shown in Figure 1C. The UV/vis

spectra collected at each point on the titration curve show the changes in the d−d spectral bands (λ_{max} = 510, 544, and 622 nm) due to the phenolate complex (Brader et al., 1990, 1997) upon replacement by the carboxylate complex (λ_{max} = 538 and 572 nm) (Figure 1A,B). In the presence of 100 mM phenol, 4H3N, with a K_{Dapp} of 0.085 mM, was found to give the tightest binding of the carboxylate anions tested in this study. The relatively high affinity of 4H3N allowed estimation of the number of binding sites from the end point of the titration (Figure 1C); the point of intersection between the initial slope and the final tangent (with a slope of 0) gives an end point value of 0.71 mM 4H3N for 0.34 mM Co^{2+}-insulin hexamer, corresponding to a stoichiometry of two binding sites per hexamer.

In order to compare the relative binding affinities of various anions to that of the Co^{2+}-R_6 hexamer, changes in the d−d bands of the Co^{2+} center (Figure 1) were used as the signal for the replacement of coordinated phenolate ion by the carboxylate ion. Substitution of Co^{2+} for Zn^{2+} at the HisB10 site provides a useful optical probe for this displacement assay (Figure 1) (Roy et al., 1989; Brader et al., 1990, 1991; Brader & Dunn, 1990; Gross & Dunn, 1992; Bloom et al., 1995; Choi et al., 1993, 1996). The d−d transition signatures of the Co^{2+}-R_6 phenolate adduct are characterized by peaks at 508, 544, and 622 nm with molar absorptivities of 230, 300, and 410 M^{-1} cm^{-1}, respectively (Figure 1A,B) (Brader et al., 1991). Although most of the aromatic carboxylate anions give rise to a similar envelope of transitions, with peaks at 536 and 572 nm, and molar absorptivities of <350 M^{-1} cm^{-1} (Figure 1B, curve b), some of the aromatic carboxylate anions, e.g., 3-nitrobenzoic acid and the fatty acid carboxylates, do not give peaks at 572 nm but show instead a small shoulder at this wavelength (Figure 1B, curve c). When these data were plotted as a function of the free ligand concentration (eq 1), we found that each titration curve could be fit to the positive lobe of a rectangular hyperbola (Figure 2), indicating identical and independent sites.

The apparent dissociation constants (K_{Dapp}) determined through the above-described procedure are listed for a wide variety of organic carboxylates in Table 1. The data given in Table 1 show that the affinity for fatty acids increases with increasing chain length. The longest fatty acid tested, lauric acid (C_{12}), gave the tightest binding, with a K_{Dapp} of 0.5 mM. The K_{Dapp} values for the different aromatic carboxylate derivatives tested (Table 1) show molar absorptivites of <280 M^{-1} cm^{-1}. The most tightly binding ligand in this class is 4H3N, with a K_{Dapp} of 0.085 mM. The weakest binding is coumalate, with a K_{Dapp} of 9.85 mM. Carboxylates with large ring systems such as indole-3-carboxylate and 4-*trans*-(*N*,*N*-dimethylamino)cinnamate also show favorable binding to the His(B10) metal sites, with a K_{Dapp} of <1 mM. Benzoic acid derivatives with hydrophilic substituents at the meta and para positions showed lower K_{Dapp} values in comparison with benzoic acid alone, while benzoic acid derivatives with substitution on the ortho position gave higher K_{Dapp} values.

The ^{1}H NMR spectra presented in Figure 1D exhibit signatures which establish that in the presence of phenol the carboxylates give R_6 complexes with the Zn(II)-substituted hexamer. These signatures include the upfield-shifted resonances previously identified as the C-4 proton of HisB5 (∼5.7 ppm), the TyrB16 ring 3,5 protons (∼6.3 ppm), and

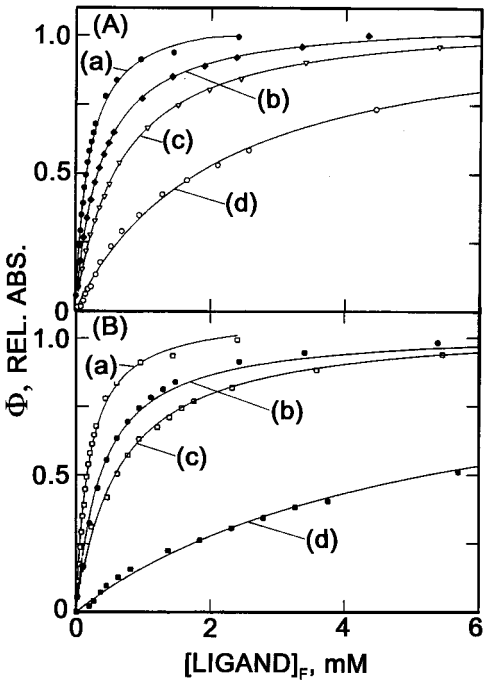

FIGURE 2: Isothermal binding curves showing the dependence of the relative absorbance, Φ, on the free ligand concentration for the binding of organic carboxylates to the Co(II)-R_6 insulin hexamer: (A) (a) 3-nitrobenzoate, (b) 3-hydroxybenzoate, (c) 3-aminobenzoate, and (d) isophthalate and (B) (a) 3-nitrobenzoate, (b) benzoate, (c) 3,5-dinitrobenzoate, and (d) 2-methyl-3-nitrobenzoate.

the TyrB26 ring 3,5 protons (∼6.6 ppm). The chemical shifts of the TyrB16 and TyrB26 3,5 ring protons identify these complexes as R_6 species, not T_3R_3 species (Brzovic et al., 1994). These spectra also include resonances from the carboxylate ligands. For 3-nitrobenzoate, the free ligand shows a set of sharp resonances at 7.70, 8.30, 8.50, and 8.80 ppm. Resonances corresponding to bound ligand are located at 8.60 and 8.75 ppm. The 4-hydroxy-3-nitrobenzoate system shows resonances for the free ligand at 7.70, 8.28, and 8.45 ppm and resonances for the bound species at 7.75 and 8.40 ppm. The detection of separate, well-defined resonances for both the free and bound carboxylates indicates that the rate of exchange is intermediate to slow on the NMR time scale for these ligands. Similar spectra were obtained for some of the aliphatic carboxylate complexes (including adamantanecarboxylate, trimethylacetate, acetate, propionate, and nonanoate) (data not shown). These spectra show that, for each carboxylate examined, the complex formed has the signatures of the R_6 structure. These data, taken together with the UV/vis absorbance studies with both the zinc- and cobalt-substituted hexamers, gave no indication that carboxylate binding to T_3 sites is significant under the experimental conditions reported in this work.

Optical Probes of Ligand Binding to the Zn(II)-R_6 Hexamer. The bound ligands, 4H3N and 4-nitro-3-hydroxybenzoate, have broad, intense, $\pi-\pi^*$ electronic transitions in the range of 400−520 nm (ϵ_{410} = 4.3 × 10^3 M^{-1} cm^{-1} and ϵ_{422} = 4.1 × 10^3 M^{-1} cm^{-1}). The use of these ligands in concentrations of >0.5 mM, with 1.00 cm path length cuvettes, gives optical densities that exceed the detection limits of the UV/vis spectrometer. Therefore, a reverse strategy was employed to determine the isotherms for the binding of these two chromophoric ligands to the Zn^{2+}-R_6 hexamer. By varying the concentration of the phenolate Zn^{2+}-R_6 complex while maintaining a constant ligand

Table 1: Comparison of Apparent Dissociation Constants for Ligand Binding to the HisB10 Sites of the Co(II)- and Zn(II)-Substituted R_6 Insulin Hexamers with Ligand pK_a and Hammett σ Values

ligand	pK_a	σ[f]	K_{Dapp}[g] (mM) Co(II)	K_{Dapp}[g] (mM) Zn(II)	ratio[h]
aliphatic carboxylates					
dodecanoate			0.5		
nonanate	4.96[a]		1.1		
octanoate	4.89[a]		1.3		
heptanoate	4.89[a]		1.6		
valerate	4.86[b]				
propionate	4.88[b]		20		
acetate	4.76[b]		37.6	17	2.2
trimethylacetate	5.01[b]		3.5		
1-adamantanecarboxylate			0.8	0.45	1.8
aromatic carboxylates					
3-nitro-4-hydroxybenzoate			0.08	0.05	1.6
3-indoleacrylate			0.15		
4-amino-3-hydroxybenzoate	4.93[c]		0.22		
p-trans-(*N*,*N*-dimethylamino)cinnamate			0.24		
3-nitrobenzoate	3.47[a]	0.71	0.25	0.16	1.6
4-hydroxybenzoate	4.58[b]	−0.37	0.36	0.19	1.9
4-aminobenzoate	4.92[a]	−0.66	0.39	0.21	1.9
indole-3-carboxylate	3.87[c]		0.44		
4-acetamidobenzoate	4.28[d]		0.48		
nicotinate	4.75[d]		0.49		
4-methylbenzoate	4.34[b]	−0.17	0.49		
benzoate	4.19[a]	0.00	0.50	0.27	1.9
3-hydroxybenzoate	4.08[b]	−0.12	0.51	0.29	1.8
3-amino-4-hydroxybenzoate			0.56		
3-hydroxy-4-nitrobenzoate			0.59	0.39	1.5
3-aminobenzoate	4.78[a]	−0.16	0.64	0.42	1.5
3,5-dinitrobenzoate	2.85[d]		0.65		
4-hydroxycinnamate			0.76		
β-3-pyridylacrylate			0.86		
4-(trifluoromethyl)benzoate		0.54	0.99		
3-nitrocinnamate	4.05[d]		1.02		
2-naphthylacetate	4.17[b]		1.57		
isonicotinate	4.86[d]		1.79		
isophthalate	3.46[b]	0.37	2.17		
	4.46[b,e]				
urocanate			2.22		
4-*tert*-butylbenzoate	4.40[b]	−0.20	2.86		
4-(*N*,*N*-dimethylamino)benzoate	5.03[b]	−0.83	3.02		
4-(hydroxyphenyl)acetate			4.01		
2-methyl-3-nitrobenzoate			5.05		
coumalate			9.85		
inorganic anions					
chloride			10.4	0.35	30
thiocyanate			0.02	0.02	10

[a] Values taken from Linde (1993). [b] Values taken from Sober and Harte (1970). [c] Values taken from Buckingham and Macdonald (1996). [d] Values taken from Dean (1992). [e] First and second pK_a values. [f] Values taken from Lowry and Richardson (1976) and March (1977). [g] Values measured as described in the text in 50 mM Tris-perchlorate buffer at pH 8.00 and 25 °C. Values are estimated to be in error by no more than ±15%. [h] Values calculated as the apparent dissociation constant measured for the Co(II)-substituted complex divided by the apparent dissociation constant measured for the Zn(II)-substituted complex.

concentration (0.1 mM), we observed the spectral shift resulting from binding as the ligand is converted from the free to the bound species (Figure 3A,B). Subtraction of the bound spectrum from the free spectrum for 4H3N yields a difference spectrum with a characteristic minimum at 444 nm (Figure 3A, curve c), while 4-nitro-3-hydroxybenzoate gives a difference spectrum with a minimum at 472 nm (data not shown). Monitoring the increasing optical density values at these wavelengths gives titration curves that can be used to determine both the stoichiometry of binding and K_{Dapp}. The titration curve for the binding of 4H3N gave a stoichiometry of one ligand per HisB10 metal site (Figure 4A). To further verify the assumption that all of the carboxylate ions coordinate to the same binding site, a plot of 1/absorbance vs 1/ $[L]_{free}$ was constructed (data not shown). All of the curves were linear, and all were found to converge on the same y-intercept value as the x values approached zero, indicating that all of the carboxylate anions directly displace 4H3N from a single class of binding sites.

K_{Dapp} values for the two chromophores, 4H3N and 4-nitro-3-hydroxybenzoate, were found to be 0.05 and 0.38 mM, respectively (Figure 4B). The Co^{2+}-substituted insulin hexamer results establish that all of the carboxylate anions studied bind to the HisB10 metal ion. Therefore, the red-shifted spectrum of 4H3N bound to the metal site (Figure 3) provides a useful spectroscopic probe for studying the binding affinities of nonchromophoric ligands to Zn^{2+}-R_6. Titrations involving displacement of this chromophoric ligand by other nonchromophore ligands were used to determine the binding affinities of the nonchromophoric ligands toward the Zn^{2+}-substituted HisB10 metal sites. The resulting titration curves were analyzed by the equation $\Phi =$

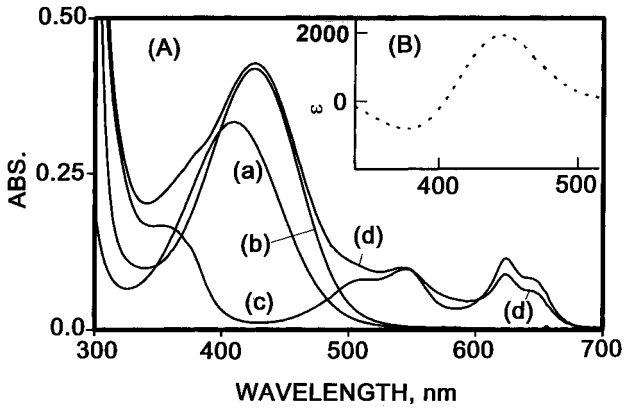

FIGURE 3: (A) UV/vis spectra showing the effects of HisB10 coordination on the spectrum of 4H3N: (a) free 4H3N, (b) 4H3N bound to the Zn(II)-R_6 hexamer, (c) the Co(II)-R_6 phenolate complex, and (d) 4H3N bound to the Co(II)-R_6 hexamer. (B) Difference spectrum (bound − free) for the binding of 4H3N to Zn(II)-R_6.

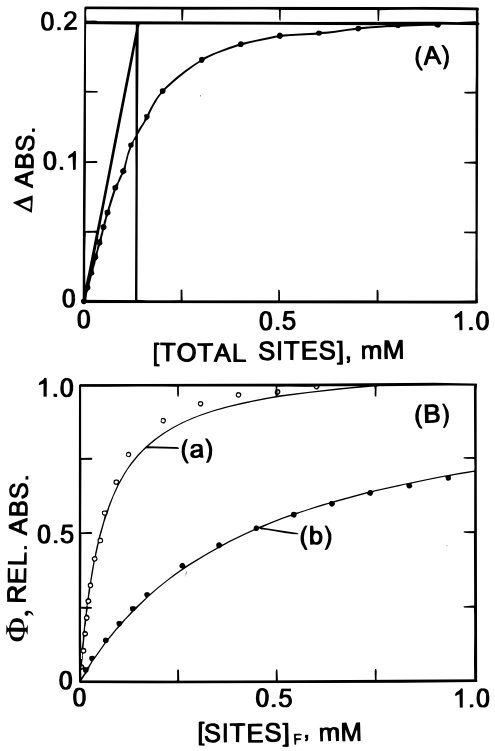

FIGURE 4: (A) Titration of 0.1 mM 4H3N with the Zn(II)-R_6 hexamer in the presence of 100 mM phenol. The titration end point (0.13 mM) defined as the *x*-intercept of the initial and final tangents to the curve gives a binding stoichiometry for 4H3N:metal ion sites of approximately 1.0:1.0. (B) Titrations showing the dependence of the relative absorbance, Φ, for the binding of the Zn(II)-R_6 hexamer to 4H3N (a) and to 4-nitro-3-hydroxybenzoate (b) measured by the red-shifted spectra of the complexes (viz. Figure 3).

$(\Phi_{max}[\text{ligand}]_F)/(K_D^{Obs} + [\text{ligand}]_F)$, where the subscript F refers to the free ligand concentration and the relative absorbance values refer to measurements obtained using the spectral changes of 4H3N. This equation has the same form as eq 1 with one modification. The apparent dissociation constant of the nonchromophoric ligand is measured in competition with the chromophore ligand. Consequently, an internally consistent set of K_{Dapp} values for the nonchromophoric ligands was obtained from the relationship $K_D^{Obs} = K_{Dapp}(1 + [I]/K_{4H3N})$, where [I] is the total concentration of the chromophore ligand and K_{4H3N} is the apparent dissociation constant of the chromophoric ligand measured in the presence of 100 mM phenol. The K_{Dapp} values determined for eight monosubstituted benzoate derivatives are listed in Table 1. As before, the tightest binding carboxylate is 4H3N.

DISCUSSION

The physicochemical properties of the insulin hexamer are remarkably dependent on the structure and nature of the ligands bound to this allosteric protein. The preparation of insulin formulations for use in the treatment of type I (insulin-dependent) diabetes is critically dependent on the modulation of the allosteric state of the hexamer by ligand binding (Brange, 1978). Knowledge at the molecular level concerning the allosteric properties of insulin, the nature of the effector sites, and the mechanism of the allosteric transition has only recently been obtained (Kaarsholm et al., 1989; Derewenda et al., 1989; Roy et al., 1989; Brader et al., 1991; Brzovic et al., 1994; Bloom et al., 1995; Choi et al., 1993, 1996; Birnbaum et al., 1996; Rahuel-Clermont et al., 1997). Herein, we extend the technology available for the quantification of ligand interactions in the insulin hexamer, and we show that organic carboxylates comprise a large class of allosteric effectors that are of potential use as stabilizing ligands, and therefore may be suitable candidates for designing improved formulations of insulin for the treatment of diabetes.

UV/Vis Spectral Properties of the Co(II)-R_6 Insulin Hexamer Carboxylate Complexes. The d−d electronic transitions of the Co(II)-substituted insulin hexamer (Figure 1) are sensitive both to the coordination geometry of the metal center and to the nature of the coordinating ligands (Roy et al., 1989; Brader et al., 1990, 1991, 1992a; Gross & Dunn, 1992; Choi et al., 1993, 1996; Brzovic et al., 1994; Bloom et al., 1995). This sensitivity to the ligand field makes the Co(II)-substituted species the system of choice for investigating ligand binding properties and allosteric behavior. The T-state Co(II)-substituted HisB10 sites are characterized by a broad, featureless, low-intensity envelope of d−d transitions centered at ∼500 nm, consistent with an octahedral $Co(II)N_3O_3$ ligand field (N = His imidazolyl, O = H_2O) (Blundell et al., 1972; Cotton & Wilkinson, 1972; Earnshaw & Harrington, 1973; Lever, 1986; Roy et al., 1989; Choi et al., 1996). The spectra of Co(II)-substituted R-state complexes display d−d transitions located between 500 and 600 nm consisting of narrow, relatively intense bands with energies modulated by the electronic properties of the fourth ligand (Figure 1A,B). These spectra are consistent with distorted tetrahedral and pentacoordinate ligand field geometries (Lever, 1986; Brader et al., 1990, 1991, 1992a, 1997). The signatures of structure present in the NMR spectra shown in Figure 1D identify the complexes formed as R_6 species (Brzovic et al., 1994). No evidence was found indicating that any of the carboxylates studied bind to or compete with the binding of ligands to the phenolic pockets.

Organic Carboxylates Give Five-Coordinate Complexes. Brader et al. (1991, 1997) have shown that the R-state complexes with simple monovalent anions such as the halides and pseudohalides give spectra that are classic examples of tetrahedral Co(II) complexes with the composition $Co(II)N_3L$, where L is the exogenous, fourth ligand (Scheme 1B). Brader et al. (1991, 1997) also have shown that small

bidentate ligands (such as pyridine-2-thiolate and acetate) appear to be capable of forming complexes which either are five-coordinate or are distorted tetrahedral with interactions from a more remote fifth ligand. Glusker (1991) has reviewed data contained in the Cambridge Structural Database (Allen et al., 1979) to determine the preferred geometries of metal ion−ligand bonding. Her analysis shows that, in small molecule complexes, Zn(II) has a strong preference for in-plane syn coordination to one oxygen of the carboxylate group, a result in agreement with the greater basicity of the syn lone pair vs the anti lone pair (Gandour, 1981; Rebek et al., 1986). However, in-plane anti coordination occurs fairly frequently, while complexes where both oxygens of the carboxylate are coordinated with similar bond lengths to the metal center are rare. In Zn-metalloproteins with Glu or Asp carboxylate ligands, syn coordination is strongly preferred over anti (Christianson, 1991). Complexes in which both oxygens of a carboxylate are close enough to the metal center to qualify as bonded have been observed in several zinc proteins, including a thermolysin carboxylate inhibitor complex (Monzingo & Matthews, 1984), carboxypeptidase (Rees et al., 1983; Christianson & Lipscomb, 1987), and alkaline phosphatase (Kim & Wyckoff, 1991).

The cobalt d−d spectra obtained for each of the organic carboxylate complexes examined in this study exhibit energies and intensities consistent with assignment of the complexes either as pentacoordinate or as distorted tetrahedral with a weak interaction to a distant fifth ligand. These organic carboxylates fall into two spectroscopic categories: those which yield UV/vis absorption spectra with two well-defined λ_{max} peaks located at 536 and 572 nm and those with a single λ_{max} peak located at 536 nm and a shoulder in the 570 nm region (Figure 1B). While the spectral differences between these two categories are small, we conclude that the differences must arise from an alteration in geometry due to a changed orientation of the carboxylate ligand with respect to the Co(II)N_3 system. This alteration in geometry could reflect either an altered Co−O bond length or a rotation of the carboxylate plane with respect to the trigonal Co(II)-N_3 framework. Such a rotation would alter orbital interactions between the carboxylate π system and the cobalt d orbitals.

The large rearrangement in the d−d transitions of the R-state Co(II) center that occurs when phenolate is replaced by an organic carboxylate (Figure 1A,B) provides a sensitive optical signal for measuring the binding stoichiometry and affinity of the carboxylate relative to phenolate (Figure 2, Table 1). The stoichiometry of carboxylate binding was established as one per site (two per hexamer) by an end point titration (Figure 1C) using 4H3N (the carboxylate with the highest affinity identified in these studies). The K_{Dapp} values (Table 1) afford a basis for correlating carboxylate structure with affinity. As expected, these data show that the nature of the organic moiety attached to the carboxylate functionality influences the affinity for the HisB10 site.

Principles of Ligand Design for the HisB10 Site. The R-state HisB10 sites consist of a metal center (substituted with Co^{2+} or Zn^{2+} in these studies) situated on the hexamer 3-fold symmetry axis about 12 Å down from the surface to the bottom of a tunnel which, together with the metal ion, forms the binding site for monovalent anions (Scheme 1B,C). The tunnel surface is constructed of the side chain residues contributed by each of the three N-terminal B-chain helices

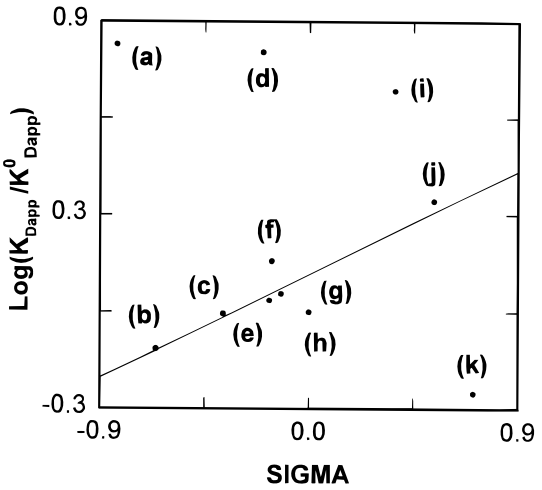

FIGURE 5: Hammett sigma-rho analysis of substituent effects on the binding of substituted benzoates to the Co(II)-R_6 hexamer. The slope of the straight line fit ($\rho = 0.35$, $r^2 = 0.804$) to the data (excluding a, d, i, and k) indicates that electron-releasing substituents meta or para to the carboxylate can enhance the affinity for the HisB10 site. The substituents tested are as follows: (a) 4-$N(CH_3)_2$, (b) 4-NH_2, (c) 4-OH, (d) 4-*tert*-butyl, (e) 4-CH_3, (f) 3-NH_2, (g) 3-OH, (h) H (benzoate), (i) 3-CO_2H, (j) 4-CF_3, and (k) 3-NO_2. Data taken from Table 1. All σ values were taken from Lowry and Richardson (1976), except for the value for 4-*tert*-butylbenzoate which was taken from March (1977).

of an R_3 unit bundled together about the 3-fold axis. The tunnel inner walls are predominantly hydrophobic with potential polar and/or hydrogen bonding loci provided by the side chain amido groups of AsnB3. The X-ray structures of various R_6 and T_3R_3 species (Derewenda et al., 1989; Smith & Dodson, 1992a,b; Ciszak & Smith, 1994; Whittingham et al., 1995) show that there is considerable flexibility in the N terminus portion of these helix bundles. This flexibility allows side chain conformations to adapt to the specific structure of the ligand. For example, in the phenolate complex (Smith & Dodson, 1992a), the AsnB3 side chains rearrange to make a cap over the entrance to the tunnel, enclosing phenolate within the tunnel (viz. Scheme 1C). In other structures, the AsnB3 side chains are rotated away from the 3-fold axis, making a more open entrance to the tunnel.

An obvious first design criterion concerns the strength of the bonding between the carboxylate and the metal center. Zn(II) and Co(II) are classified as Lewis acids on the borderline between "hard" and "soft" (Cotton & Wilkinson, 1972) and, thus, exhibit low polarizability and low covalency in bonding interactions with hard bases such as carboxylate oxygen (Glusker, 1991; Dunn, 1995). Zn−O and Co−O bonds are primarily electrostatic; hence, bond strengths are dominated by charge densities on the coordinating ligand and at the metal center. Therefore, electron-donating substituents which increase the density of negative charge on the carboxylate (via inductive or resonance effects) will increase the electrostatic component of the bonding interaction. The Hammett sigma-rho relationship (Figure 5) provides a means of evaluating benzoic acid derivatives to determine the extent to which the electron-releasing properties of substituents on the ring correlate with the affinity of the ligand for the HisB10 site. When all of the data points are plotted assuming the applicability of the Hammett sigma-rho relationship, there appears to be no obvious correlation.

If a more restricted set of data consisting of the carboxylates with small para substituents (e.g., 4-NH_2, 4-OH, 4-CH_3, 4-H, and 4-CF_3 together with the 3-NH_2 and 3-OH derivatives) is considered, then the plot with the line indicated in Figure 5 suggests that charge density can make an important contribution to carboxylate affinity. However, as will be discussed later, steric and hydrophobic interactions appear to be of equal or greater importance. The slope of the best-fit straight line drawn (excluding the values for 4-(*N*,*N*-dimethylamino)benzoate, 4-*tert*-butylbenzoate, isophthalate, and 3-nitrobenzoate) gives a ρ value of 0.35. The large positive and negative deviations shown by 4-(*N*,*N*-dimethylamino)benzoate, 4-*tert*-butylbenzoate, isophthalate, and 3-nitrobenzoate (Figure 5) likely are due to interactions between the substituent and the walls of the tunnel. Although the σ values for 4-(*N*,*N*-dimethylamino)benzoate and 4-aminobenzoate (PABA) are similar (−0.83 and −0.66, respectively), the K_{Dapp} values for these compounds differ by 8.7-fold, indicating that the binding of the 4-(*N*,*N*-dimethyl) derivative is weakened by an unfavorable interaction of the methyl groups with the tunnel surface. This unfavorable interaction could be steric or electrostatic. The more bulky methyl groups could introduce steric clashes. The replacement of N-H by N-CH_3 undoubtedly alters H bonding interactions with the ligand; if the 4-amino group of PABA is H bonded to the protein, then replacement of H by CH_3 will alter this interaction. Since the Hammett plot identifies the *N*,*N*-dimethyl derivative as the outlier, unfavorable steric interactions seem to be the more likely explanation. This conclusion is reinforced by the finding that the value for 4-*tert*-butylbenzoate shows a strong deviation from the value predicted by the Hammett correlation. The σ values for 4-*tert*-butylbenzoate and 4-methylbenzoate (−0.20 and −0.17, respectively) are nearly identical, yet the K_{Dapp} values for these ligands differ by 5.8-fold. Therefore, the weaker binding of the 4-*tert*-butyl derivative almost certainly is due to a clash between the *tert*-butyl group and the tunnel surface. The 4-fold-enhanced affinity of 3-nitrobenzoate over that predicted by the Hammett correlation likely reflects favorable dipolar and/or van der Waals interactions between the nitro group and the tunnel wall. Due to the electron-withdrawing effect of the nitro group nitrogen, the nitro oxygens are extremely poor H bond acceptors.[2] Therefore, significant weak bonding interactions between the nitro group and nonaromatic side chain groups on the protein are dominated by dipolar interactions or van der Waals contacts.

The data presented in Table 1 for the fatty acids indicate that hydrophobic interactions make a significant contribution to ligand affinity at the HisB10 site. These data show that affinity increases with increasing chain length, with K_{Dapp} values ranging from 37.6 mM for acetate ion to 0.5 mM for laurate ion, a 75-fold range in affinity. The incremental change in the free energy of binding for the series of fatty acids shown in Table 1 (−0.13 to −0.6 kcal/mol per added methylene group at 25 °C) is typical of a hydrophobic interaction.

[2] This is true for ring systems lacking a strong electron-releasing group ortho or para to the nitro group. The placement of a hydroxyl group or an amino group ortho to the nitro group, as in 4H3N, or 4-nitro-3-hydroxybenzoate, brings about a significant increase in the electron density of the nitro group oxygens, rendering them H bond acceptors.

Because the tunnel is oriented along the hexamer 3-fold symmetry axis (Scheme 1), the HisB10 site has a unique symmetry that can be exploited in the design of ligands. For this reason, carboxylate ligands with a β-C exhibiting 3-fold symmetry, i.e.,

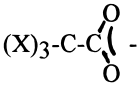

and suitably tailored substituents, X, were investigated as ligands for the HisB10 site. The dissociation constants measured for the series $X_3 = H_3$, $(CH_3)_3$, and 1-adamantanyl (Table 1) decrease from 37.6 mM (acetate), to 3.5 mM (trimethylacetate), to 0.80 mM (adamantane-1-carboxylate). This trend indicates that ligand affinity is strongly influenced by the steric bulk of the β-C substituents. Molecular modeling (data not shown) indicates that the trimethyl and adamantanyl moieties make favorable van der Waals contacts with the hydrophobic surface of the tunnel.

Examinations of the X-ray structures of T_3R_3 and R_6 species (Smith et al., 1984; Smith & Dodson, 1992a; Whittingham et al., 1995) show that the side chain amide of AsnB3 is able to assume an orientation where H bonding interactions could be formed between the side chain amide donor and acceptor substituents on the ligand. Evidence of such interactions is indicated by the relatively high affinities of 4H3N, its 4-nitro-3-hydroxy isomer, and 4-amino-3-hydroxybenzoate (Table 1). Figure 6A presents the results of molecular modeling studies exploring possible modes of binding for 4H3N. This stereodiagram shows one of three identical orientations of 4H3N in which the carboxylate group forms a five-coordinate complex with the metal center with O−Zn bonds of unequal length. In this particular complex, the side chain $(CH_3)_2CH$ group of LeuB6 makes van der Waals contact with the hydrogen at the 2-position of the 4H3N ring, and the more distant oxygen of the carboxylate is positioned within H bonding distance of the backbone NH of CysB7. Rotation of the carboxamide side chain group of AsnB3 would bring it within H bonding distance of the nitro oxygens and/or phenolic oxygen of 4H3N. Figure 6B presents a CPK space filling model of the same 4H3N complex viewed from the top looking down the 3-fold symmetry axis. From inspection of this model, it is clear that, while 4H3N has a steric bulk that nicely spans the cavity, the 3-fold symmetry of the cavity does not allow a snug fit to the planar structure of this ligand, and therefore, 4H3N does not completely fill the cavity. Clearly, an appropriately tailored ligand with substituents matching the 3-fold symmetry of this site could optimize van der Waals contacts and H bonding interactions with the protein.

4-Hydroxy-3-nitrobenzoate (4H3N) Is a Chromophoric Probe of Ligand Binding to the HisB10 Site. The pK_a of the phenolic hydroxyl of 4H3N is 6.41 (Buckingham & Macdonald, 1996). Consequently, at the pH of these studies (pH 8.0), this group is essentially completely ionized. When 4H3N coordinates to the HisB10 site of an R_3 unit, the spectrum of the ortho nitrophenylate chromophore is shifted to longer wavelengths, and the magnitude of the shift is sensitive to the nature of the metal ion (Figure 3). The data presented in Figure 3 and Table 1 show that, when used as a chromophoric indicator, 4H3N provides a sensitive probe of ligand binding to the HisB10 site that can be exploited to

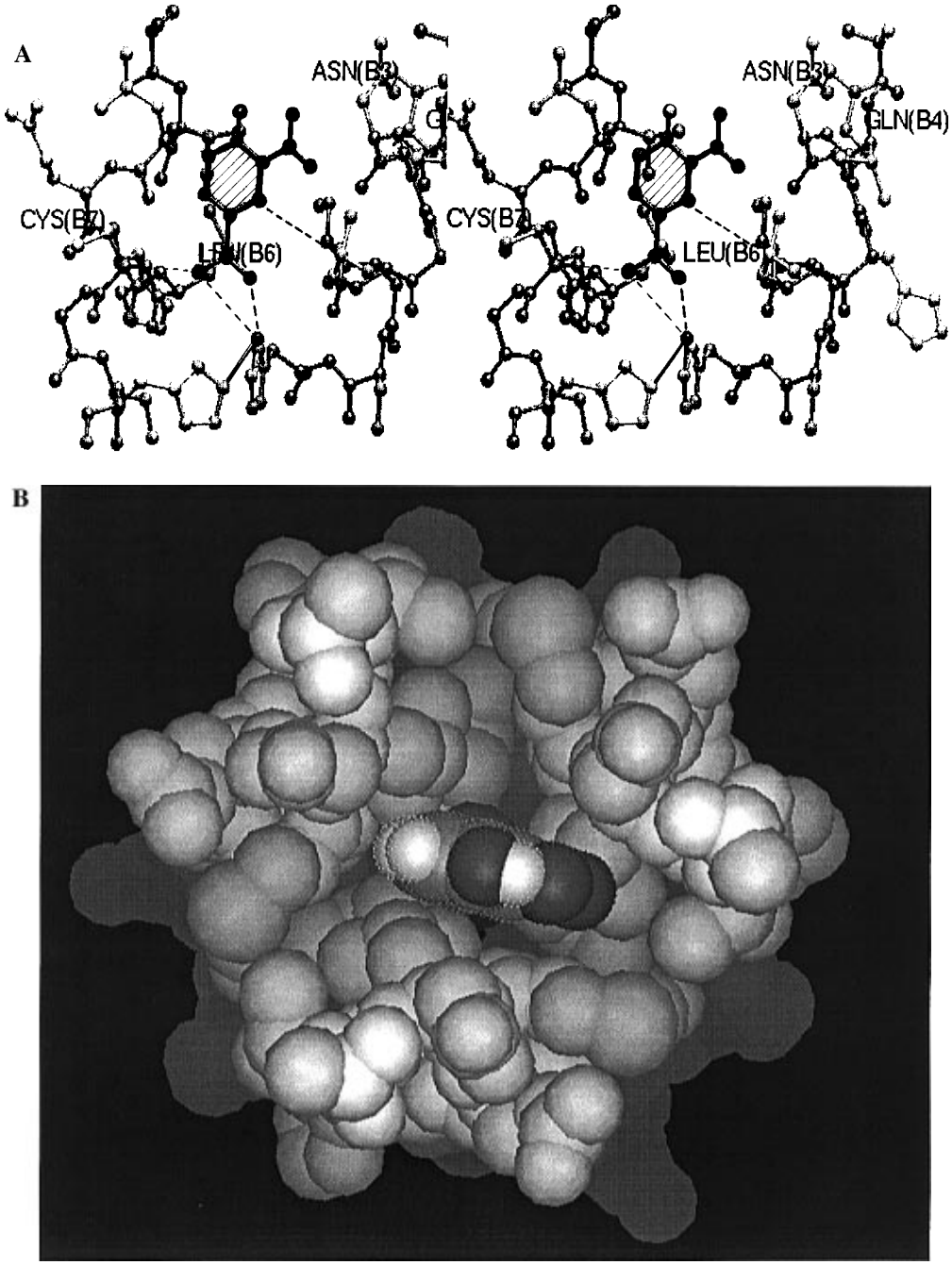

FIGURE 6: (A) Stereodiagram showing the results of modeling the structure of 4H3N into the HisB10 binding site of an R_3 unit. The site is viewed perpendicular to the 3-fold axis, with one subunit of an R_3 unit cut away to reveal interactions between the site and the ligand. In this model, 4H3N is depicted in an asymmetric five-coordinate structure with unequal distances (dashed lines) between the two carboxylate oxygens and the metal ion. The more distant oxygen is positioned within H bonding distance of the amide NH of CysB7 (dashed line). In this orientation, the ortho position of 4H3N makes van der Waals contact with the side chain methyl group of a LeuB6 residue (dashed line). In the hexamer structure used in this modeling exercise, the AsnB3 side chains are rotated away from the ligand. Inspection of the model shows that the nearest AsnB3 carboxamide group could be rotated to a position allowing H bonds to the ligand nitro and/or hydroxyl oxygens. (B) CPK space filling model of an R_3 unit with 4H3N bound to the HisB10 site viewed from the top along the 3-fold symmetry axis. The modeling in panels A and B is based on the structure of the Zn(II)-R_6 chloride ion complex (Smith & Dodson, 1992a) (coordinates provided courtesy of G. D. Smith).

determine the relative affinities of ligands for Zn(II)-substituted R-state hexamers. Because previously described methods for evaluating binding to the Zn(II)-insulin hexamer are relatively inconvenient and insensitive (e.g., ^{1}H NMR, CD, and differential microcalorimetry), the use of 4H3N as a probe provides an important new method that is highly sensitive and convenient both for monitoring ligand binding to the HisB10 sites of R-state complexes and for determining the isotherms for the T to R allosteric transition induced by phenolic ligands (C. R. Bloom, N. Wu, A. Dunn, N. C. Kaarsholm, and M. F. Dunn, in preparation).

Metal Ion Effects on the Affinity of the HisB10 Site. Comparison of the apparent dissociation constants obtained for the Co(II)- and Zn(II)-substituted R_6 species using the same series of carboxylates (Table 1 and Figure 7) indicates that the Zn(II) complex has a slightly higher affinity than does the Co(II) complex by a factor of ~1.8. Since the R_6 complex with phenol bound to the phenolic pockets and

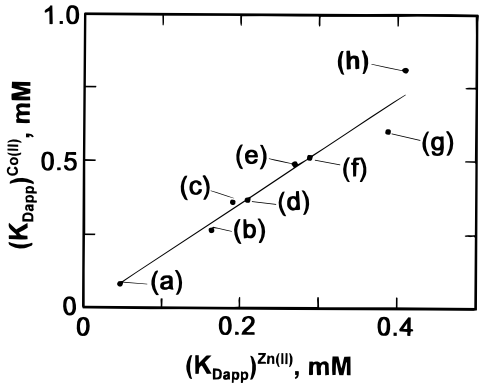

FIGURE 7: Comparison of metal ion substitution on carboxylate affinity. The best fit straight line has a slope of 1.77. Ligands are as follows: (a) 4H3N, (b) 3-nitrobenzoate, (c) 4-hydroxybenzoate, (d) 4-aminobenzoate, (e) benzoate, (f) 3-hydroxybenzoate, (g) 4-nitro-3-hydroxybenzoate, and (h) adamantane-1-carboxylate. Data taken from Table 1.

phenylate coordinated to the HisB10 metal ion is used as the reference state for both data sets, the thermodynamics of the T to R transition are not a factor in this comparison. However, differences in the relative affinities of Co(II) vs Zn(II) for phenylate ion likely are a contributing factor. When the comparison is extended to Cl^- and SCN^-, the apparent metal ion effect is much larger (Table 1), the apparent affinity of the Zn(II) complex for SCN^- is tighter by ~10-fold, while the apparent affinity for Cl^- is tighter by ~30-fold. Since Co^{2+} and Zn^{2+} are nearly identical in size, the higher affinity of Zn(II) for these ions likely is due to differences in the electronic structures of these metal centers.

Conclusions. This work shows that organic carboxylates comprise an interesting new class of allosteric ligands for the HisB10 metal sites of the R-state insulin hexamer with affinities which greatly exceed those of the ligands (i.e., acetate ion and chloride ion) currently used to stabilize insulin formulations based on the T_3R_3 and R_6 conformational states of the insulin hexamer. It further is shown that suitably selected chromophoric carboxylates such as 4H3N or substituted cinnamates provide optical signals which can be exploited as (a) probes of ligand binding to R_3 units of the hexamer and (b) indicators of the T- to R-state conformational transition in the insulin hexamer (C. R. Bloom, N. Wu, A. Dunn, N. C. Kaarsholm, and M. F. Dunn, in preparation).

ACKNOWLEDGMENT

We are indebted to G. David Smith for providing the coordinates of the Zn(II)-R_6 chloride complex we used in modeling the binding of carboxylates to the HisB10 sites.

REFERENCES

Allen, F. H., Bellard, S., Brice, M. D., Cartwright, B. A., Doubleday, A., Higgs, H., Hummelink, T., Hummelink-Peters, B. G., Kennard, O., Motherwell, W. D. S., Rodgers, J. R., & Watson, D. G. (1979) *Acta Crystallogr., Sect. B 35*, 2331−2339.

Baker, E. N., Blundell, T. L., Cutfield, J. F., Cutfield, S. M., Dodson, E. J., Dodson, G. G., Hodgkin, D. C., Hubbard, R. E., Isaacs, N. W., Reynolds, C. D., Sakabe, K., Sakabe, N., & Vijayan, N. M. (1988) *Philos. Trans. R. Soc. London, Ser. B 319*, 369−456.

Birnbaum, D. T., Dodd, S. W., Saxberg, B. E. H., Varshavsky, A. D., & Beals, J. M. (1996) *Biochemistry 35*, 5366−5378.

Bloom, C. R., Choi, W. E., Brzovic, P. S., Ha, J. J., Huang, S.-T., Kaarsholm, N. C., & Dunn, M. F. (1995) *J. Mol. Biol. 245*, 324−330.

Blundell, T., Dodson, G., Hodgkin, D., & Mercola, D. (1972) *Adv. Protein Chem. 26*, 279−402.

Brader, M. L., & Dunn, M. F. (1990) *J. Am. Chem. Soc. 112*, 4585−4587.

Brader, M. L., & Dunn, M. F., (1991) *Trends Biochem. Sci. 16*, 341−345.

Brader, M. L., Kaarsholm, N. C., & Dunn, M. F. (1990) *J. Biol. Chem. 265*, 15666−15670.

Brader, M. L., Kaarsholm, N. C., Lee, R. W.-K., & Dunn, M. F. (1991) *Biochemistry 30*, 6636−6645.

Brader, M. L., Borchardt, D., & Dunn, M. F. (1992a) *J. Am. Chem. Soc. 114*, 4480−4486.

Brader, M. L., Borchardt, D., & Dunn, M. F. (1992b) *Biochemistry 31*, 4691−4696.

Brader, M. L., Kaarsholm, N. C., Harnung, S. E., & Dunn, M. F. (1997) *J. Biol. Chem. 272*, 1088−1094.

Brange, J., Skelbaek-Pedersen, B., Langkjaer, L., Damgaard, U., Ege, H., Havelund, S., Heding, L. G., Jørgensen, K. H., Lykkeberg, J., Markussen, J., Pingel, M., & Rasmussen, E. (1987) in *Subcutaneous Insulin Therapy: Galenics of Insulin Preparations* (Berger, M., Ed.) Chapter 3, pp 1−71, Springer-Verlag, Berlin.

Brzovic, P. S., Choi, W. E., Borchardt, D., Kaarsholm, N. C., & Dunn, M. F. (1994) *Biochemistry 33*, 13057−13069.

Buckingham, J., & Macdonald, F., Eds. (1996) *Dictionary of Organic Compounds*, 6th ed., Chapman and Hall, New York.

Choi, W. E., Brader, M. L., Aguilar, V., Kaarsholm, N. C., & Dunn, M. F. (1993) *Biochemistry 32*, 11638−11645.

Choi, W. E., Borchardt, D., Kaarsholm, N. C., Brzovic, P. S., & Dunn, M. F. (1996) *Proteins: Struct. Funct. Genet. 26*, 377−390.

Christianson, D. W. (1991) *Adv. Protein Chem. 42*, 281−355.

Christianson, D. W., & Lipscomb, W. N. (1987) *J. Am. Chem. Soc. 109*, 5536−5538.

Ciszak, E., & Smith, G. D. (1994) *Biochemistry 33*, 1512−1517.

Cotton, F. A., & Wilkinson, G. (1972) in *Advanced Inorganic Chemistry*, 3rd ed., pp 555−619, Wiley-Interscience, New York.

Dean, J. A., Ed. (1992) *Lang's Handbook of Chemistry*, 14th ed., McGraw-Hill.

Derewenda, U., Derewenda, Z., Dodson, E. J., Dodson, G. G., Reynolds, C. D., Smith, G. D., Sparks, C., & Swensen, D. (1989) *Nature 338*, 594−596.

Derewenda, U., Derewenda, Z., Dodson, E. J., Dodson, G. G., Bing, X., & Markussen, J. J. (1991) *J. Mol. Biol. 220*, 425−433.

Dodson, E. J., Dodson, G. G., Hubbard, R. E., Moody, P. C. E., Turkengurg, J., Whittingham, J., Xiao, B., Brange, J., Kaarsholm, N., & Thϕgersen, H. (1993) *Philos. Trans. R. Soc. London, Ser. A 345*, 153−164.

Dunn, M. F. (1995) Catalytic Mechanisms in Zinc Enzymes, in Hand-Book on Metal-Ligand Interactions in Biological Fluids (Berthon, G., Ed.) pp 352−359, Marcel Dekker, Inc.

Earnshaw, A., & Harrington, T. J. (1973) *The Chemistry of the Ttransition Elements*, Claredon Press, Oxford.

Gandour, R. D. (1981) *Bioorg. Chem. 10*, 169−176.

Glusker, J. P. (1991) *Adv. Protein Chem.* ***42***, 1−76.

Gross, L., & Dunn, M. F. (1992) *Biochemistry 31*, 1295−1301.

Holyer, R. H., Hubbard, C. D., Kettle, S. F. A., & Wilkins, G. R. (1966) *Inorg. Chem. 5*, 622−625.

Kaarsholm, N. C., Ko, H.-C., & Dunn, M. F. (1989) *Biochemistry 28*, 4427−4435.

Kim, E. E., & Wyckoff, H. W. (1991) *J. Mol. Biol. 218*, 449−464.

Lever, A. B. P. (1986) *Inorganic Electronic Spectroscopy*, Elsevier Publishing Co., New York.

Linde, D. R., Ed. (1993) *CRC Handbook of Chemistry and Physics*, 74 ed., CRC Press, Boca Raton, FL.

Lowry, T. H., & Richardson, K. S. (1976) *Mechanism and Theory in Organic Chemistry*, p 62, Harper and Row, New York.

March, J. (1977) *Advanced Organic Chemistry, Reaction Mechanisms, and Structure*, p 253, McGraw-Hill, New York.

Monzingo, A. F., & Matthews, B. W. (1984) *Biochemistry 23*, 5724−5729.

Porter, R. R. (1953) *Biochem. J. 53*, 320−328.
Rahuel-Clermont, S., French, C. A., Chou, C. I., Kaarsholm, N. C., & Dunn, M. F. (1997) *Biochemistry 36*, 5837−5845.
Rebek, J., Jr., Duff, R. J., Gordon, W. E., & Parris, K. (1986) *J. Am. Chem. Soc. 108*, 6068−6069.
Rees, D. C., Lewis, M., & Lipscomb, W. N. (1983) *J. Mol. Biol. 168*, 367−387.
Roy, M., Brader, M. L., Lee, R. W.-K., Kaarsholm, N. C., Hansen, J. F., & Dunn, M. F. (1989) *J. Biol. Chem. 264*, 19081−19085.
Sadtler Standard Spectra (1995−1996) Vol. 12−170, Sadtler Division, Bio-Rad Laboratories.
Seydoux, F., Malhotra, O. P., & Bernhard, S. A. (1974) *CRC Crit. Rev. Biochem. 2*, 227−257.
Smith, G. D., & Dodson, G. G. (1992a) *Biopolymers 32*, 441−445.
Smith, G. D., & Dodson, G. G. (1992b) *Proteins: Struct., Funct., Genet. 14*, 401−408.
Smith, G. D., Swenson, D. C., Dodson, E. J., Dodson, G. G., & Reynolds, C. D. (1984) *Proc. Natl. Acad. Sci. U.S.A. 81*, 7093−7097.
Sober, H. A., & Harte, R. A., Eds. (1970) *Handbook of Biochemistry*, 2nd ed., Chemical Rubber Co., Cleveland, OH.
Whittingham, J. L., Chaudhuri, S., Dodson, E. J., Moody, P. C. E., & Dodson, G. G. (1995) *Biochemistry 34*, 15553−15563.

BI9701639